AFRL-AFOSR-VA-TR-2016-0277

Experimental Investigation of Turbulence-Chemistry Interaction in High-Reynolds-Number Turbulent Partially Premixed Flames

Chenning Tong
CLEMSON UNIVERSITY

06/23/2016
Final Report

Air Force Research Laboratory
AF Office Of Scientific Research (AFOSR)/ RTA1
Arlington, Virginia 22203
Air Force Materiel Command

REPORT DOCUMENTATION PAGE

Form Approved
OMB No. 0704-0188

1. REPORT DATE *(DD-MM-YYYY)*	**2. REPORT TYPE**	**3. DATES COVERED** *(From To)*
06-25-2016	Final Report	*(From 09-30-2014 To 03-29-2016)*

4. TITLE AND SUBTITLE
[U] Experimental investigation of turbulence-chemistry interaction in high-Reynolds-number turbulent partially premixed flames

5a. CONTRACT NUMBER

5b. GRANT NUMBER
FA9550-14-1-0404

5c. PROGRAM ELEMENT NUMBER
61102F

6. AUTHOR(S)
Chenning Tong

5d. PROJECT NUMBER
2308

5e. TASK NUMBER
BX

5f. WORK UNIT NUMBER

7. PERFORMING ORGANIZATION NAME(S) AND ADDRESS(ES)

Department of Mechanical Engineering
Clemson University
Clemson, SC 29634

8. PERFORMING ORGANIZATION REPORT NUMBER

9. SPONSORING / MONITORING AGENCY NAME(S) AND ADDRESS(ES)
AFOSR/NA
875 Randolph Street
Suite 325, Room 3112
Arlington, VA 22203

10. SPONSOR/MONITOR'S ACRONYM(S)

11. SPONSOR/MONITOR'S REPORT NUMBER(S)

12. DISTRIBUTION / AVAILABILITY STATEMENT

Approved for public release, distribution unlimited

13. SUPPLEMENTARY NOTES

14. ABSTRACT

The project focused on implementing the photodissociation-based method for simultaneous two-dimensional imaging of mixture fraction and temperature in turbulent nonpremixed/partially premixed flames. Mixture fraction is an important variable in understanding and modeling turbulent mixing and turbulence-chemistry interaction, two key processes in such flames. Previous techniques are limited by one or more factors including the assumption of simplified flame chemistry, the use of non-inert tracer species, and the use of Raman scattering, thereby incapable of providing two-dimensional mixture fraction imaging in flames. Recently, a new method based on photodissociation of iodine containing species, two-photon laser-induced fluorescence (LIF) of atomic iodine, and Rayleigh scattering was developed by the PI and colleagues at Clemson University, enabling accurate simultaneous two-dimensional imaging in turbulent flames for the first time. The research activities focused on the technical issues in implementing the method, including achieving accurate iodine seeding level, eliminating the interference from LIF of molecular iodine excited at 532 nm and from OH excited at 298 nm, and determination of the system response. Two-dimensional imaging was performed in laminar and turbulent partially premixed methane flames to demonstrate the capability of the new measurement system.

15. SUBJECT TERMS

16. SECURITY CLASSIFICATION OF:			**17. LIMITATION OF ABSTRACT**	**18. NUMBER OF PAGES**	**19a. NAME OF RESPONSIBLE PERSON**
a. REPORT	**b. ABSTRACT**	**c. THIS PAGE**			Chiping Li
Unclassified	Unclassified	Unclassified	UL	24	**19b. TELEPHONE NUMBER** *(include area code)* 703 696-8478

Standard Form 298 (Rev. 8-98)
Prescribed by ANSI Std. Z39.18

Final Report: Experimental investigation of turbulence-chemistry interaction in high-Reynolds-number turbulent partially premixed flames

AFOSR Grant FA9550-14-1-0404

Principal Investigator: Chenning Tong
Department of Mechanical Engineering
Clemson University, Clemson, SC 29634-0921

June 10, 2016

1 Introduction

The objective of the project is to implement the unique technique based on photodissociation of iodine for simultaneous two-dimensional imaging of mixture fraction and temperature. These variables are important for characterizing and investigating turbulent nonpremixed/partially premixed flames and turbulence-chemistry interaction. Turbulent mixing of mixture fraction has been studied extensively [4, 14]. In a two-feed non-premixed flame, the mixture fraction is defined as:

$$\xi = \frac{Y - Y_o}{Y_F - Y_o} \tag{1}$$

where Y is a conserved quantity such as the mass fraction of any element, which is not altered by chemical reactions, and Y_F and Y_o are the values of Y in the fuel stream and in the oxidizer stream, respectively.

In spite of numerous previous efforts, measurements of mixture fraction in flames remains a challenge. Previous techniques generally fall in to two categories: Those based on the measurements of the major species and those on an inert tracer species. For the former, Raman scattering technique can be employed to obtain the mass fractions of all the major species [1, 9, 10]. However, due to the weak Raman scattering process the method is limited to one-dimensional (1D), and

consequently one-component of the scalar dissipation rate. To avoid the weak Raman signal, simplified chemistry is often assumed to reduce the number of species measured. While such techniques are capable of two-dimensional imaging, the assumption of reduced chemistry is generally not warranted and can result in large measurement errors, especially in the reaction zone. For the inert tracer-based techniques, a tracer species such as NO or acetone is seeded in the fuel stream [15, 16]. Due to the much stronger LIF signal, these techniques are capable of providing two-dimensional images of the mixture fraction. However, the use of NO is limited to dry CO flames [16], while acetone undergoes pyrolysis near the reaction zone; therefore the technique is incapable of providing the mixture fraction in the reaction zone, where it is needed the most. A more recent technique use planar laser-induced fluorescence (PLIF) of Krypton [6], but requires quenching corrections, for which two-dimensional images of all the major species are needed. Because no current measurement techniques are capable of providing two-dimensional images of the major species, their quenching effects cannot be fully corrected.

To enable simultaneous two-dimensional mixture fraction and temperature imaging under a wide range of combustion conditions, a novel technique based on the use of photo-dissociation (PD) was proposed at Clemson [18, 19, 20], which overcomes the limitations of existing measurement techniques. The generic diagnostics concept of the technique consists of two steps: the photo-dissociation of the precursor and the probing of the fragments. We have identified Iodine (I_2), which is seeded in the target flow, as an excellent precursor [18, 19, 20]. In step one, the PD laser pulse dissociates all species containing I element including I_2, HI and CH_3I; therefore I element only exists as atomic I in the flow field. Because the PD is complete, the mass fraction of these foreign I atoms represents that of the seeded precursor and forms a conserved scalar. In step two, the probing laser pulse is used to detect the number density of the atomic I, from which the mixture fraction can be inferred (in combination with Rayleigh scattering measurements, see section 3). Two-photo laser induced fluorescence (TPLIF) of iodine atoms can be used to detect atomic I. The TPLIF signal intensity is linearly proportional to the laser intensity, and is quenching free with moderate laser irradiance. Thus, this technique avoids the need for quenching corrections and

provides a unique capability to image mixture fraction in two dimensions.

As described in the above diagnostic concept, the new method overcomes the limitations inherent in the current techniques. It a) avoids using the weak Raman signals, and instead exploit the much stronger LIF signals for two-dimensional imaging, b) circumvents the need of multi-scalar measurements, thereby enjoying relative simplicity of experimental implementation and data interpretation, and c) does not rely on any assumption of simplified chemistry and does not require the precursor to remain inert, thereby enabling applications in a wide range of flame conditions and complex fuels. The description of the diagnostic concept also suggests two requirements for applying the new imaging method: a) the rapid and complete PD of the precursor and all products containing the target photofragment, and b) a technique to image the target photofragment. Our preliminary results have identified I_2 as the precursor that can satisfy these requirements for the study of hydrocarbon flame (not limited to simple fuel like CH_4).

2 Implementation of the technique

The concept of the iodine photo-dissociation based technique has been demonstrated in Zhao et al [18, 19, 20]. In this section, we discuss the experimental setup and the various technical issues in implementing the technique in non-premixed/partially premixed flames, including seeding of iodine, interference from the LIF signal of I_2 excited at 532 nm, interference from the LIF of hydroxyl (OH) excited at 298 nm, and determination of the system response.

In order to achieve sufficient signal level for the relative large flow rate in the Sandia Flames, a significant amount of iodine (approximately 0.5% of the mass flow rate) needs to be seeded in the fuel stream. Iodine is a solid at room temperatures. Hiller&Hanson [3] have shown that the seeding concentration of iodine through sublimation from iodine crystals in a simple container is within 10% of the saturation value. However, the gas flow rate in their study was much smaller than for the Sandia flames. For large gas flow rates, the iodine container needs to be heated. In the mean time, the seeding level needs to reach the saturation vapor pressure in order to achieve accurate control of the iodine mass fraction. We found that a major problem for this seeding method is

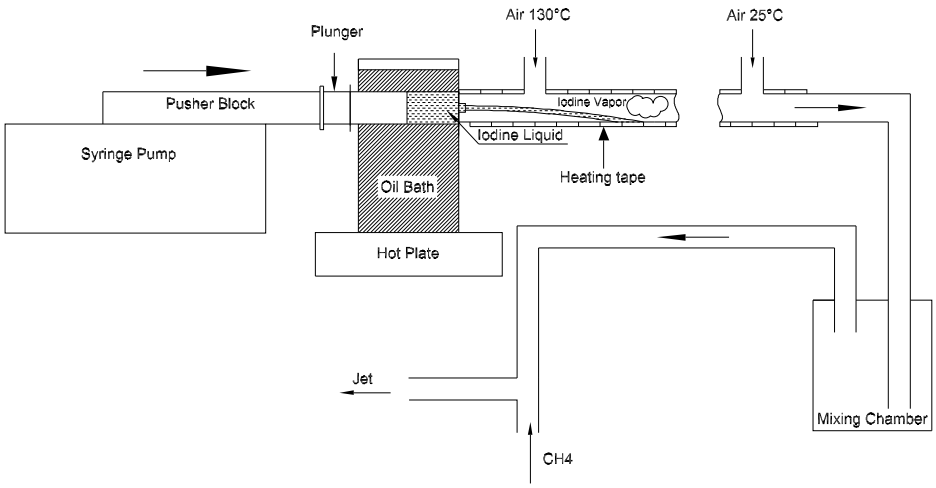

Figure 1: Schematic of the iodine seeding.

that there was significant iodine deposition along the gas flow path; therefore a fine particle filter was necessary because otherwise the iodine particles would interfere with the Rayleigh scattering imaging. However, iodine corrosion caused damage of the particle filter in a relatively short period of time and the deposition blocked the flow path. Another sublimation-based method using a fluidized-bed mixing chamber was proposed in [3], which, however, is difficult to achieve since iodine flakes tend to adhere to each other. To avoid these difficulties a different method involving liquid iodine and its evaporation is eventually employed in the present work (figure 1). We note that the melting and boiling points of iodine are at 113.7^oC and 184.3^oC, respectively. We place iodine in a glass syringe, which is surrounded by an oil bath maintained at approximately 123^oC to ensure that the iodine is in the liquid state. A syringe pump is used to accurately control the flow rate of the iodine. The liquid iodine flows out of the syringe needle to a hot surface that is maintained at approximately 185^oC, which is sufficiently high to ensure fast evaporation of the liquid iodine. It is important that the entire flow path of the liquid iodine is maintained above its melting point to prevent solidification. The seeding concentration, therefore, is insensitive to the temperature of the liquid iodine. An air flow, which is approximately 20% of the total air flow, is heated to 130^oC before flowing toward the hot surface. The iodine seeded air flow subsequently mixes with the rest of the gas flow before entering the jet tubes. Due to the length of the tubing to the burner, the temperature of the fuel stream is close to the room temperature.

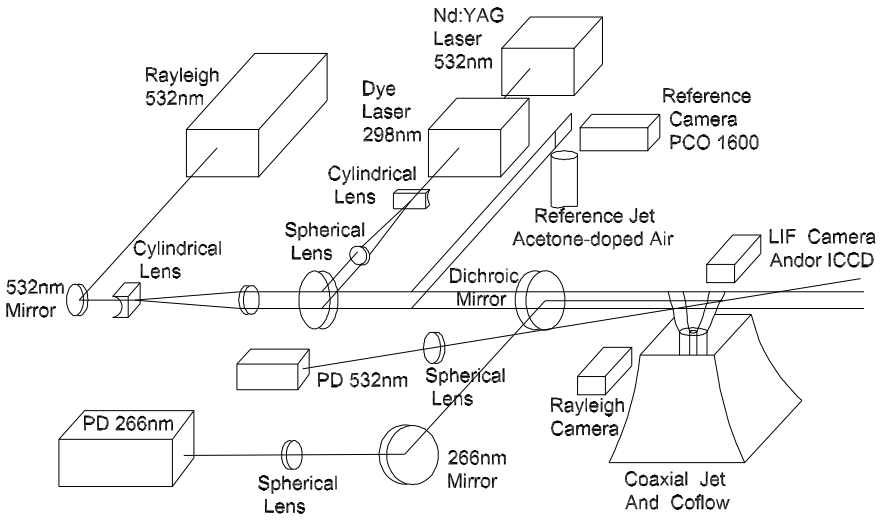

Figure 2: Schematic of the experimental setup.

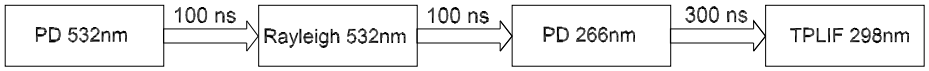

Figure 3: The timing scheme of laser pulses.

We use simultaneous TPLIF of I and Rayleigh scattering to obtain the mixture fraction and the temperature. The schematic of the experimental setup is shown in figure 2. The 298.2 nm laser pulse, generated by a dye laser pumped by the second harmonic of a Nd:YAG laser, is used for TPLIF, since atomic I has a strong two-photon LIF transition at this wavelength. The TPLIF emission is at 804 nm. The second harmonic of another Nd:YAG laser, label as "Rayleigh 532 nm", is used for Rayleigh scattering measurement. When seeded in hydrocarbon flames, I_2 results in four iodine-containing species: I_2, HI, CH_3I and atomic I. In order to use the concentration of I atoms as a conserved scalar, I_2, CH_3I and HI need to be photodissociated. Previous studies [18, 19, 20] have shown that a 266 nm laser pulse is able to dissociate all these species while a 532 nm laser pulse can only dissociate I_2. Thus a frequency-quadrupled Nd:YAG laser, label as "PD 266 nm", is used to dissociate the species. However, the effective Rayleigh cross section of the gases appear to be slightly altered by the high energy PD 266 nm laser pulse, thus the Rayleigh 532 nm pulse must arrive before the PD 266 nm pulse. Using this timing arrangement, we found that there is

a strong LIF signal of I_2 when excited at 532 nm (the Rayleigh laser pulse), which interferes with Rayleigh scattering, since I_2 has not been dissociated. A previous study [11] has shown strong fluorescence of iodine vapor excited at 532 nm. We found that the LIF signal of I_2 with the seeding level ($\approx 0.05\%$ by volume) at the saturation vapor pressure at room temperature is approximately 80% of the Rayleigh signal of pure air. In addition, there is a strong resonant fluorescence signal for I_2 excited at 532 nm [11], which is approximately 14% of the Rayleigh signal of pure air, which we determined by removing the LIF signal using a short pass filter with cut-off wavelength of 550 nm (figure 4). To eliminate these interferences another PD laser pulses, label as "PD 532 nm", is used to dissociate I_2 (figure 2). The PD 532 nm laser pulse overlaps with the other laser pulses in the field of interest. A short pass filter is used to remove any residual LIF signal (figure 2). The results show that there is no observable difference between the Rayleigh signal (from the Rayleigh 532 nm beam) of air seeded with iodine and that of pure air (figure 5). In addition the results do not depend on the time lag between the two 532 nm beams (tested between 70 ns to 1000 ns), suggesting that there is no recombination of I atoms. The timing scheme of the laser pulses is shown in figure 3. The time lag between the Rayleigh 532 nm and the TPLIF 298 nm needs to be small to ensure that the measurement can be considered simultaneous.

Previous studies [18, 19, 20] have shown that photodissociation of I_2 by the 532 nm laser only results in ground state I atoms, which can be detected by the 298.2 nm TPLIF, whereas some I atoms can enter an excited state, labeled I^*, in the process of photodissociation of I_2, HI and CH_3I by the 266 nm beam. Direct measurements of I^* using PLIF would require another laser wavelength. We avoid this complication by making use of the quenching characteristics of I^*, which becomes the ground state I through quenching. The typical quenching time scale in flames is approximately 300 ns. This time scale is much shorter than the chemical time scale in flames for I (on the order of ms). We exploit this disparity in time scales to achieve near I^*-free measurements. After the photodissociation laser pulse, I^* generated in the process will return to the ground state (I). In the mean time, this time is too short for any chemical reaction to consume I. By imaging I approximately 300 ns after the photodissociation pulse, we avoid the complication

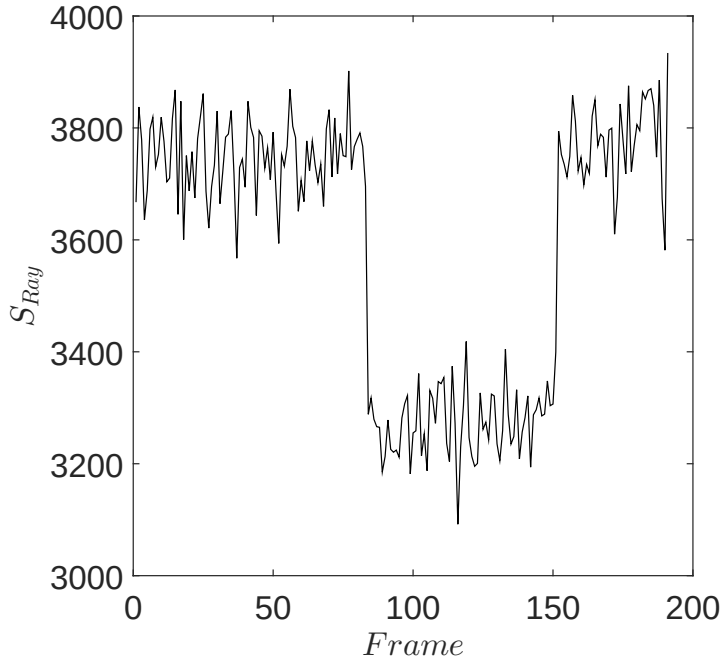

Figure 4: The signal of air seeded with iodine obtained by the Rayleigh camera. The iodine seeding is turned off at frame number of approximately 75, and turn back on at approximately 155. The signal before frame 75 and after 155 is due to both Rayleigh scattering and I_2 LIF by the 532nm excitation whereas it is pure Rayleigh scattering of air between frame 75 and 155.

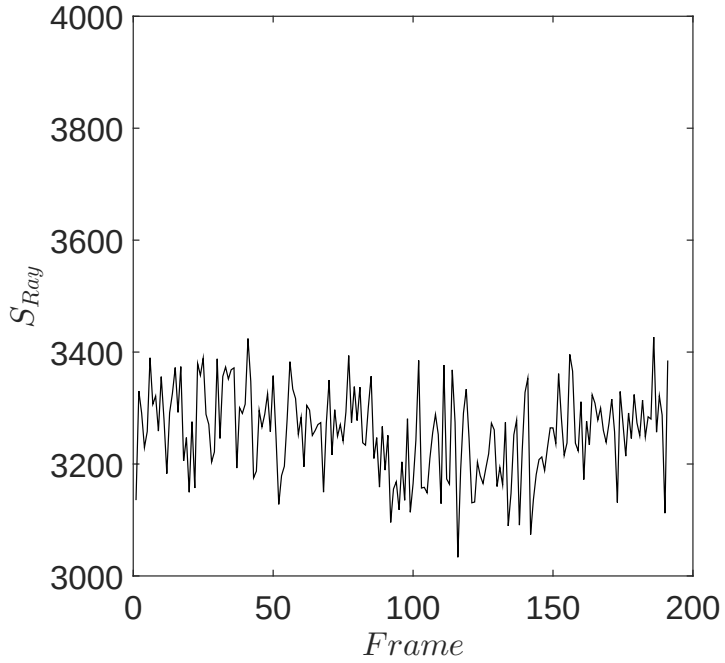

Figure 5: Condition same as figure 4 but with PD 532nm beam arriving earlier than the Rayleigh 532nm beam.

of I^* to obtain accurate measurement of I. We note that for $\xi > 0.8$, I element exists mostly as I_2 and the photodissociation of I_2 by 532 nm only results in the ground state of I atoms while I element exists mostly as I atoms due to high temperature for $\xi < 0.6$, where photodissociation is unnecessary. The mass fractions of HI and CH_3I are significant only between $0.6 < \xi < 0.7$, with the peaks near $\xi = 0.7$ where the mole fraction of I element in HI and CH_3I is about 30% of the total I element. Thus, the PD 266 nm is mostly used to photodissociate HI and CH_3I near $\xi = 0.7$. With a time lag of 300 ns between the PD 266 nm and the TPLIF 298 nm, this would result in approximately 4-5% measurement uncertainties.

Another issue we found is that the methane/air laminar flame excited by the 298.2 nm laser beam has signals near the reaction zone (figure 6) even when the flow is not seeded with iodine. The signal strength is comparable to the iodine TPLIF signal. Therefore, this signal interferes with the TPLIF signal. It is highly likely that the signal is the fluorescence of the hydroxyl radical since the $(A \leftarrow X)$ transition of OH is near 300 nm [7]. There has been previous studies of OH LIF using laser wavelength at approximately 280 nm [2], at 282.75 nm [8], at 287.9nm [13] and at 306.4 nm [12]. Since the dominant LIF signal of OH is between 300nm and 340 nm [13], which is far away from the TPLIF signal of I (804nm), it can be eliminated by placing a long-pass filter (RG780 color filter) in front of the TPLIF camera lens.

The pulse energy of the lasers are 200 mJ, 340 mJ, 220 mJ and 20 mJ, respectively, for the PD 532 nm, the Rayleigh 532 nm, PD 266 nm and the TPLIF 298 nm beams. A telescope consisting of a plano-concave cylindrical lens (FL: -500 mm) and a spherical lens (FL: 1000 mm) was placed in the beam path of the Rayleigh 532 nm beam to form a collimated laser sheet above the burner (figure 2). The telescope on the beam path of the TPLIF 298 nm also consists of a cylindrical lens with focal length of -500 mm and a spherical lens with focal lens of 1000 mm. The focal point of the spherical lens on the beam path of the Rayleigh 532 nm and the TPLIF 298 nm is above the burner. A dichroic mirror that transmits 532 nm and reflects 298 nm is used to combine the two beam paths. Another dichroic mirror that reflects 266 nm and transmits 298 nm and 532 nm is used to combined the beam path of the PD 266 nm with that of the Rayleigh 532 nm and the

TPLIF 298 nm. The PD 532nm laser pulse only overlaps with the other laser pulses in the field of interest. In order for complete dissociation of I_2 and the reaction products (HI and CH_3I) in the whole widths of the Rayleigh 532 nm beam and the TPLIF 298 nm beam, the beam widths of the PD 532nm pulse and the PD 266nm are large enough to ensure that the energy of the dissociation pulses are relatively uniform across the widths of the probing beams. Thus the focal points of the spherical lenses for the PD 532nm pulse and the PD 266nm are away from the jet.

The TPLIF signal from atomic I is collected with a Andor ICCD (DH734-18F-73), which is equipped with a custom lens arrangement consisting of a 85 mm focal length Zeiss lens followed by an Achromat with focal length of 160 mm and diameter of 80 mm. The Rayleigh signal is collected with another Andor ICCD (DH334T-18F-63), which is also equipped with a custom lens arrangement consisting of a 85 mm focal length Nikon lens followed by another Achromat with focal length of 160 mm and diameter of 80 mm. The full widths at half maximum (FWHM) of the line-spread function are approximately 38 μm and 55 μm, respectively for the TPLIF and Rayleigh cameras lens, determined by translating a razor blade across the focal plane of the camera lens [5, 17]. The exposure time of the two ICCD is less than 100 ns to suppress the effects of chemiluminescence in the flame. Both LIF and Rayleigh images of the reference jet are recorded with a PCO-1600 camera, which has a interframe transfer time of 150 ns. The registration (geometrical alignment of the images) of the cameras is performed using a fine wire to block part of the laser beam at the upstream. The locations of the shadows in the different images were used to determine the registration.

3 Data reduction procedures

The data reduction procedures to obtain the mixture fraction and the temperature from simultaneous TPLIF of iodine and Rayleigh scattering images is described in this section.

The Rayleigh signal is modeled as:

$$S_{\mathrm{Ray}} = \mathrm{Res}_{\mathrm{Ray}} \cdot I \cdot \frac{\sigma_{\mathrm{eff}}}{T} + \mathrm{BG}_{\mathrm{Ray}} \tag{2}$$

where S_{Ray}, $\mathrm{Res}_{\mathrm{Ray}}$, I, σ_{eff}, T and $\mathrm{BG}_{\mathrm{Ray}}$ are the Rayleigh signal, the system response, the laser

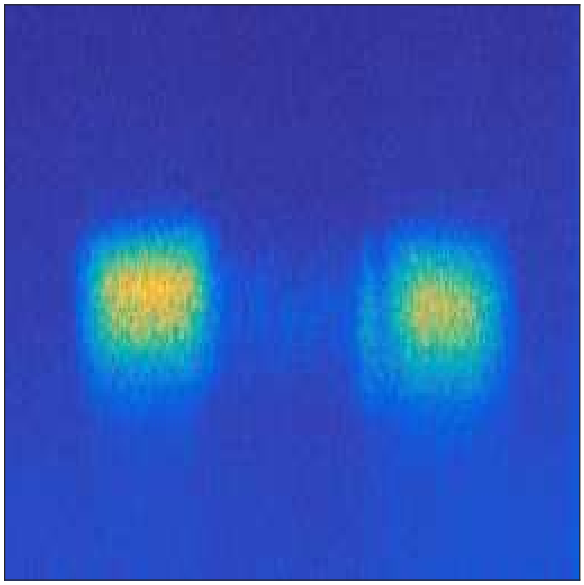

Figure 6: LIF of hydroxyl radical (OH) at 298.2 nm excitation. The center of the fuel stream is near the center of the image.

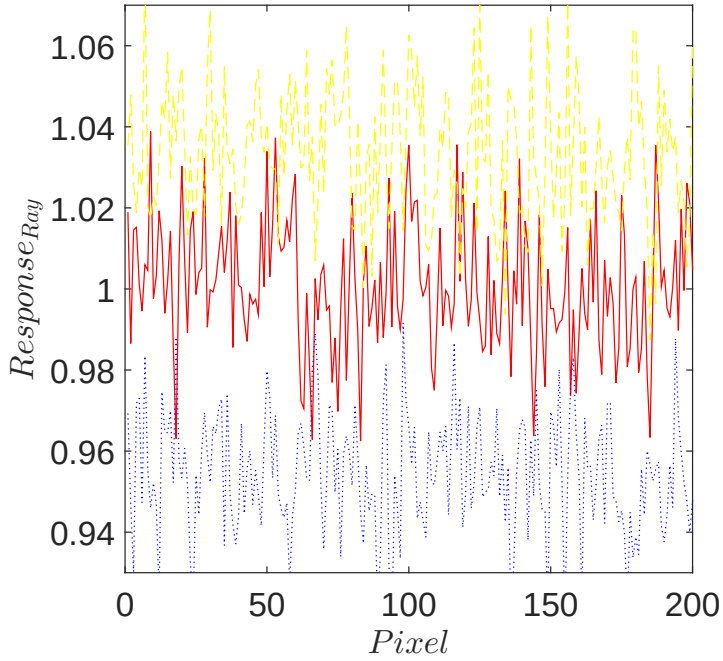

Figure 7: The ratio of three individual images responses (along a row of pixels) and the averaged response with the reference jet placed at the upstream of the main jet.

intensity, the effective Rayleigh cross section, the temperature, and the background signal, respectively.

The $\mathrm{Res_{Ray}}$ term (obtained through calibration) includes all factors that are independent of the laser intensity and the scalar values: the solid angle of the collection optics, the quantum efficiency of the camera, and the lens vignetting et al. We use a reference jet (a air flatfield) to monitor the laser beam profile and the response is obtained. However, the results show large variations (figure 7) of the responses obtained from different laser pulses if the reference jet is placed at the upstream (along the beam path) of the burner, where the laser beam is unfocused. We suspect that there is some interference of the laser light when the beam is focused, and the pulse-to-pulse variations of beam profile cause different interference patterns and thus large variations of the response. We eliminate this problem by placing a wedged window in the beam path to reflect about 6% of the 532 nm beam as the reference beam, which focused in the same manner as the beam toward the burner. The reference jet is placed at the focal point of the reference beam. Although the Rayleigh signal intensity of the reference jet is much smaller, the variations of the response term (figure 8) is greatly reduced although not been completely eliminated.

To ensure that the irradiance of the 298 nm laser beam is sufficiently large so that the LIF signal is proportional to the laser intensity (i.e., to ensure negligible quenching effects), in the present work we use a small laser beam height of 700 μm with a usable portion of 150 μm where the LIF signal is proportional to the laser intensity (figure 9). Larger beam height can be used with an increased 298 nm beam energy. The two photon LIF signal of atomic I can be modeled as:

$$S_{\mathrm{LIF}} = \mathrm{Res_{LIF}} \cdot I_{\mathrm{LIF}} \cdot \xi \cdot \rho + \mathrm{BG_{LIF}} \tag{3}$$

where S_{LIF}, $\mathrm{Res_{LIF}}$, I_{LIF}, ξ, ρ and $\mathrm{BG_{LIF}}$ represent the LIF signal, the system response for LIF, the laser intensity, the mixture fraction, the density and the background signal, respectively. The $\mathrm{Res_{LIF}}$ can be obtained in the same way as $\mathrm{Res_{Ray}}$, with the reference jet providing a stable laminar acetone-doped air flow. The laser intensity can also be monitored by sampling the 298 nm beam before combing with the 532 nm beam, and placing a uv absorption glass at the focal point of the sampled beam. A CCD camera is then used to record the fluorescence from the uv absorption glass,

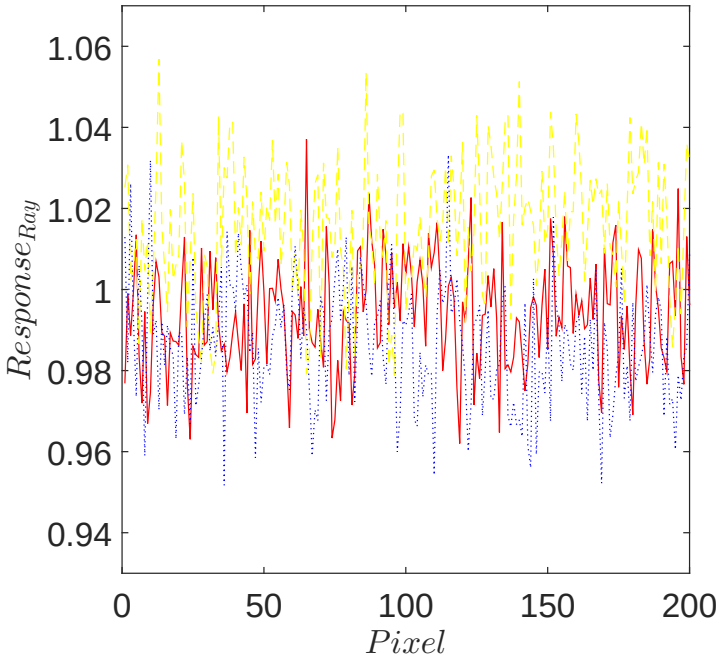

Figure 8: The ratio of three individual images responses (along a row of pixels) and the averaged response with the reference jet placed at the focus of the sampled 532 nm beam.

which is proportional to the laser intensity when the laser energy is below some threshold value.

In addition to the number density of atomic I (or mole fraction, X), the mixture density is needed to determine the iodine mass fraction (the mixture fraction). Common practices to obtain density include: 1) monitoring the concentration of all major species, which typically requires the use of Raman scattering and limits the measurements to one dimension (not applicable to the present technique), 2) using specially designed fuel and oxidizer such that the Rayleigh scattering cross-section remains relatively constant. However, such specially designed "Rayleigh friendly" flames may only have limited practical relevance.

We have determined experimentally that the Rayleigh scattering cross-section (σ_{eff}) and mixture density (ρ) in the Sandia flames depend (deterministically) only on mixture fraction and temperature to a very high degree of accuracy, i.e. $\sigma_{\text{eff}} = \sigma_{\text{eff}}(\xi, T)$ and $\rho = \rho(\xi, T)$, even under the condition of local extinction and reignition. The mixture fraction is proportional to the iodine number density and the mixture density ($\xi \propto X\rho$). With these relationships, both mixture fraction

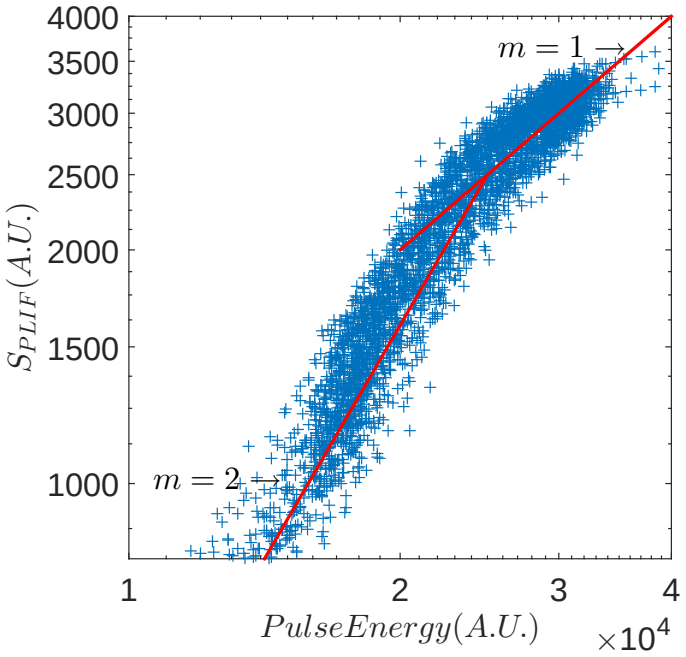

Figure 9: Linearity of iodine two-photon LIF. The scatter points are the experimental data while the two straight lines with m=1 and 2, respectively, represent that of $S_{\mathrm{LIF}} \propto I_{\mathrm{LIF}}$ and $S_{\mathrm{LIF}} \propto I_{\mathrm{LIF}}^2$, respectively.

and temperature can be obtained from the measured iodine number density and Rayleigh scattering signals. The use of the fact that the Rayleigh scattering cross-section and mixture density depend only on mixture fraction and temperature avoids the strong assumption of the two-step chemistry assumption used in previous studies. These dependencies also hold in the DLR flames and are likely to be valid in a wide range of flames. We use the Sandia flame C, D and E data of Barlow and Karpetis [9, 10] to obtain the dependence of σ_{eff} and ρ on ξ and T in the form of look-up tables (figure 10).

The LIF signal is proportional to the mixture fraction and density, $S_{\text{LIF}} \propto \xi\rho$ (equation 3). We determine the constant of proportionality by matching our data to those of Barlow and Karpetis [9, 10], the mixture fraction and temperature can then be obtained from the look-up tables for calculating $(\xi\rho, \frac{\sigma_{\text{eff}}}{T})$. We show in figure 11 the scatter plot of $(\xi\rho, \frac{\sigma_{\text{eff}}}{T})$ using the Sandia flame C data (orange). Also shown is the domain of the look-up tables in the $\xi\rho$ and $\frac{\sigma_{\text{eff}}}{T}$ spaces (blue) obtained from Sandia flame C, D and E data (with extrapolation in temperature space). The region with the lowest $\frac{\sigma_{\text{eff}}}{T}$ values corresponds to the stoichiometric mixture fraction.

To examine the quality of the LIF and Rayleigh signals, we show in figure 12 a scatter plot of $(S_{\text{LIF}}, S_{\text{Ray}})$ for a laminar flame. The general trends of the signals are similar to $(\xi\rho, \frac{\sigma_{\text{eff}}}{T})$ shown in figure 11, indicating that the signals are well behaved. There are some significant differences probably because the flame structures of the laminar flame and the turbulent flames are quite different. Another factor that can contribute to the differences is the differential diffusion between iodine and the combustion species in the laminar flame since iodine has a smaller diffusivity [19]. The effects of differential diffusion would become weaker at higher Reynolds numbers. The scatter points appear to be in clusters for large values of S_{LIF} (> 0.6) due to the discrete nature of the pixels. Figure 13 shows the scatter plot of $(S_{\text{LIF}}, S_{\text{Ray}})$ obtained in a turbulent flame with a flow velocity approximately 60% of the center jet velocity of the Sandia flame C. The overall trends are much closer to those shown in figure 11. The scatter is broader than those in figure 11, which is likely a result of several factors including the lower signal-to-noise ratio (SNR), laser intensity profile variations, beam steering, and possibly the fluctuations of the dye laser spectrum. The

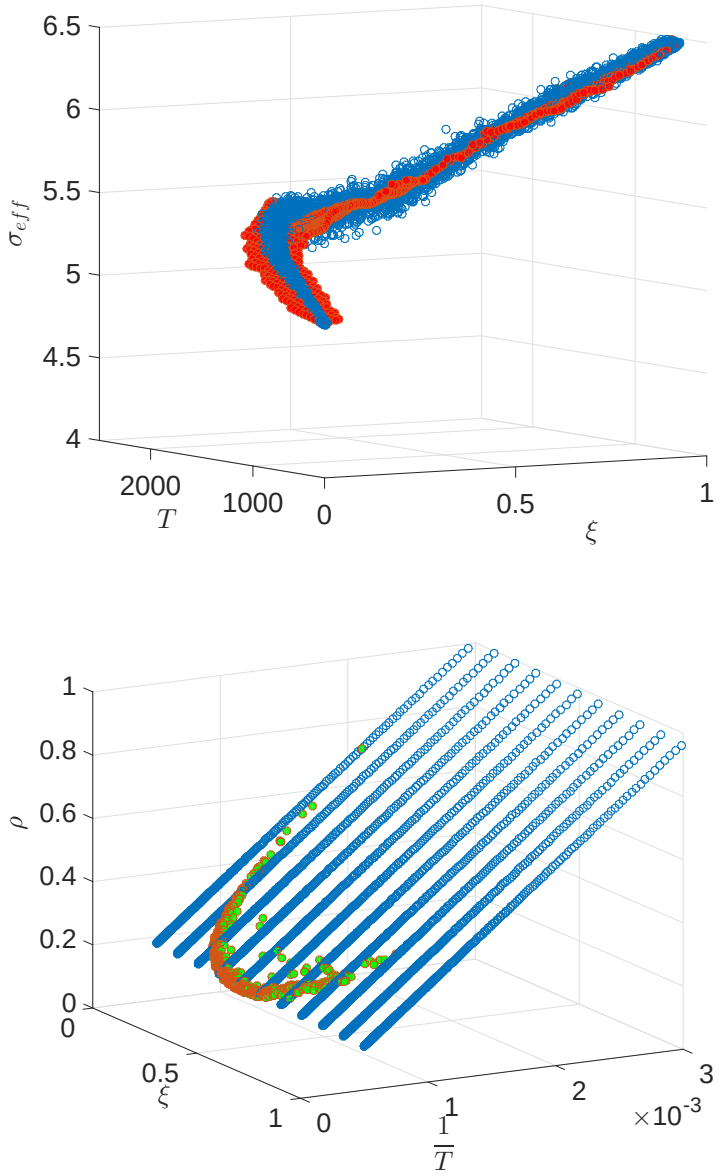

Figure 10: The dependence of σ_{eff} (Top) and ρ (Bottom) on ξ and T.

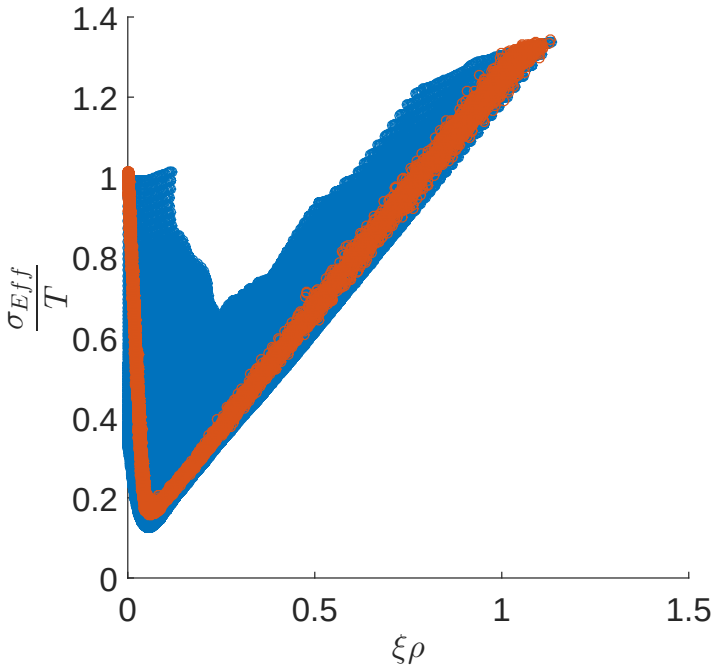

Figure 11: Scatter plot of $(\xi\rho, \frac{\sigma_{\text{eff}}}{T})$ using the Sandia flame C data (Barlow and Karpetis [9, 10]) only (orange) and using Sandia flame C, D and E data (Barlow and Karpetis [9, 10]) and with extrapolation in temperature space (blue).

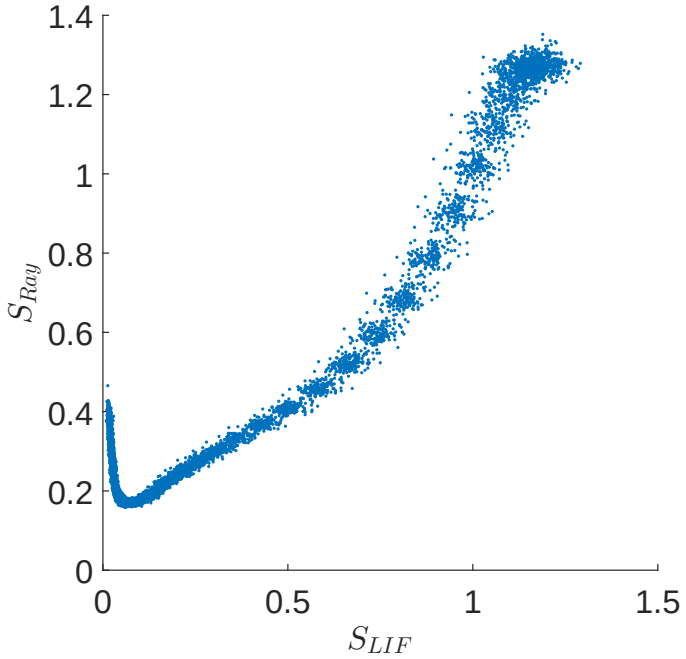

Figure 12: Scatter plot of $(S_{\mathrm{LIF}}, S_{\mathrm{Ray}})$ for a laminar flame.

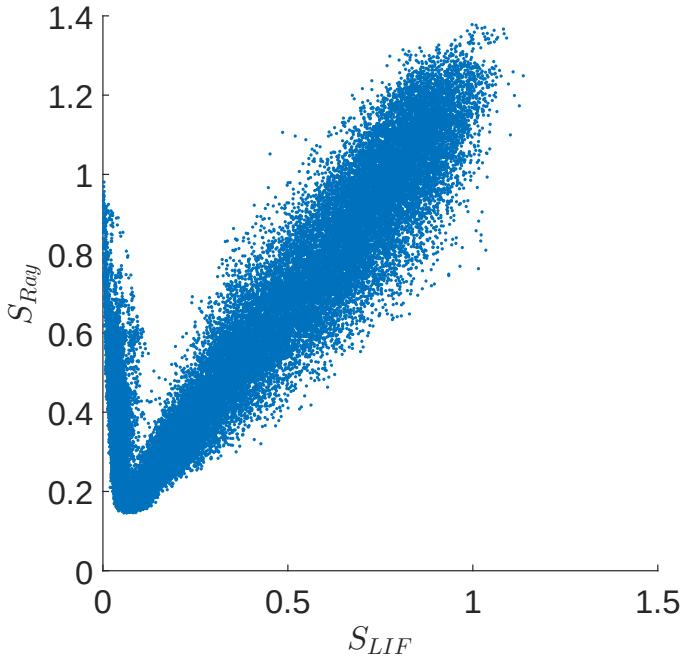

Figure 13: Scatter plot of $(S_{\mathrm{LIF}}, S_{\mathrm{Ray}})$ for a turbulent flame.

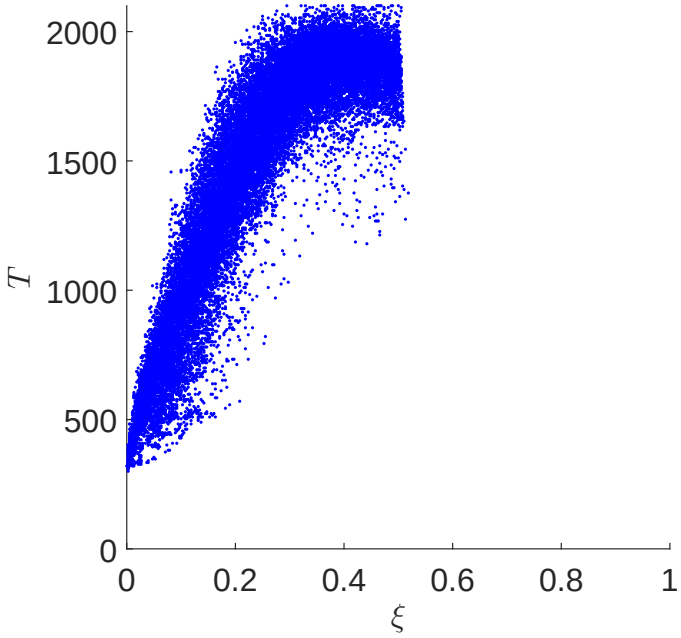

Figure 14: Scatter plot of (ξ, T) for a turbulent flame.

effects of these factors may be stronger for small beam sizes. Due to the large variations of gas density and thus the refractive index in a flame, beam steering can play a relatively larger role in the case of small beam sizes, resulting in high sensitivity of the measurement to the beam location. The effects of laser intensity profile fluctuations are also stronger when the beam size is small. Due to the two photon nature of the TPLIF of atomic iodine and the simple structure of the I atom, the signal is very sensitive to the laser wavelength. Thus the measurement is sensitive to the stability of the grating in the dye laser, which may degrade over time. Figure 14 is a scatter plot of (ξ, T) obtained for $\xi < 0.6$. We do not show the richer samples due to the large scatter. Figure 15 shows the instantaneous profiles of ξ and T for the turbulent flame.

4 Summary and future improvements

In the present work we implemented the photodissociation-based technique proposed by Zhao et al [18, 19, 20] to simultaneously image mixture fraction and temperature in two-dimensions in non-premixed flames. The new technique avoids the requirement to measure all major species

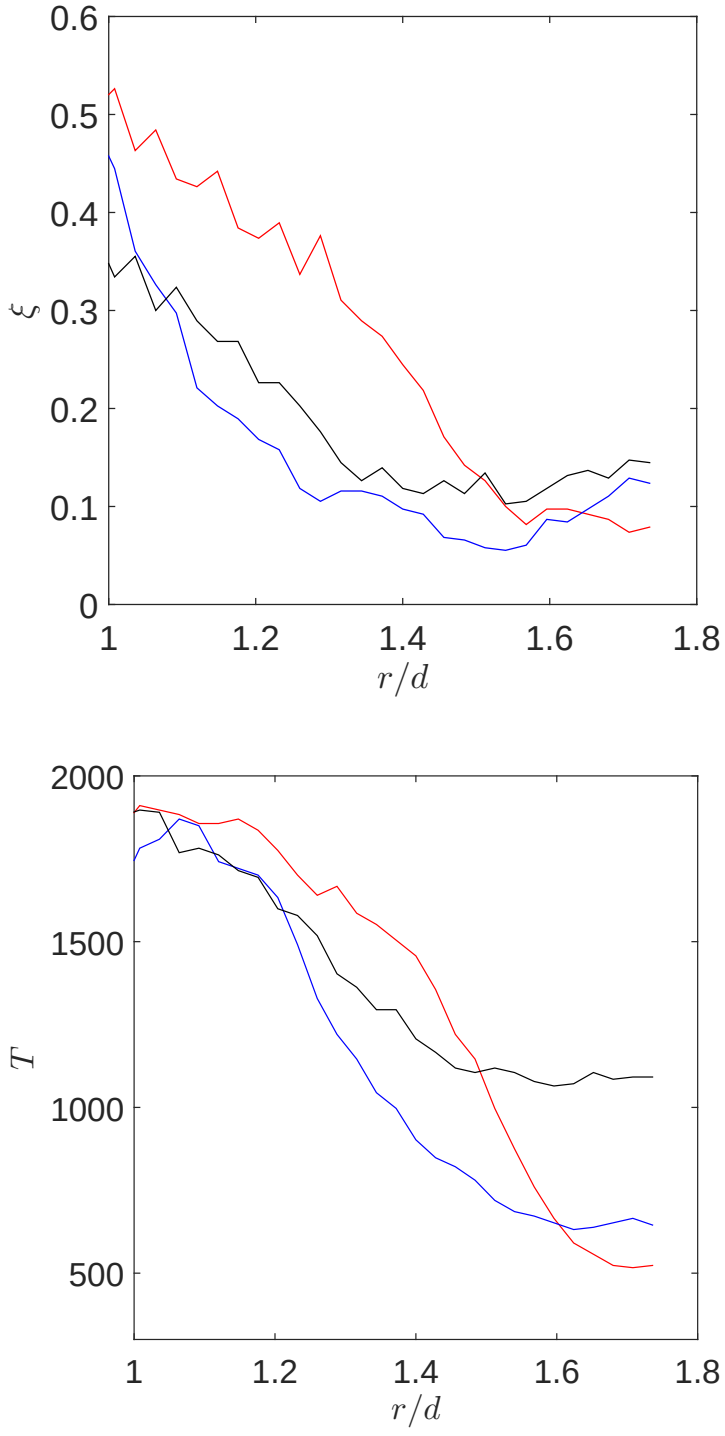

Figure 15: Line profiles of ξ and T for a turbulent flame.

for Raman-based techniques, and does not require quenching correction and the assumption of reduced chemistry. It is therefore applicable to a wide range of flame conditions. A number of technical issues were resolved in this work, including achieving a stable seeding level for iodine, the interference from the LIF signal of molecular iodine (excited at 532nm) with the Rayleigh scattering measurement, the interference from OH LIF signal with the TPLIF of I, and improved quantitative characterization of the system response. The technique was demonstrated in both laminar and turbulent non-premixed flames.

The present work also suggests several areas for future improvement: 1) improved optics for cameras to achieve higher SNR. 2) Improved telescope in the path of the 298.2 nm beam to achieve a relative large (usable) beam height so that the measurement is less sensitive to the beam steering and the laser profile variations. 3) The measurement may be sensitive to the laser spectrum fluctuations, which are related to the performance of the dye laser. The grating in the dye laser is the likely cause of the fluctuations of the laser spectrum, and will be the focus for improving the spectral stability.

References

[1] R. S. Barlow and A. N. Karpetis. Measurements of scalar variance, scalar dissipation, and length scales in turbulent piolted methane/air jet flames. *Flow, Turb. Combust.*, 72:427–448, 2004.

[2] B.Atakan, J.Heinze, and U.E.Meier. Oh laser-induced fluorescence at high pressures: spectroscopic and two-dimensional measurements exciting the a-x (1,0) transition. *Appl. Phys.*, pages 585–591, 1997.

[3] B.Hiller and R.K.Hanson. Properties of the iodine molecule relevant to laser-induced fluorescence experiments in gas flows. *Experiments in Fluids.*, 10:1–11, 1990.

[4] R. W. Bilger. The structure of diffusion flames. *Combust. Sci. Tech.*, 13:155–170, 1976.

[5] Noel T. Clemens. *Flow Imaging.* Encyclopedia of Imaging Science and Technology, 2002.

[6] A.G. Hsu, V. Narayanaswamy, N.T. Clemens, and J.H. Frank. Mixture fraction imaging in turbulent non-premixed flames with two-photon lif of krypton. *Proceedings of the combustion institute.*, 33:759–766, 2011.

[7] Mark J.Dyer and David R. Crosley. Two-dimensional imaging of oh laser-induced fluorescence in a flame. *Optics Letters.*, 7:8, 1982.

[8] O. Johansson, J. Bood, B. Li, A. Ehn, Z.S. Li, Z.W. Sun, M. Jonsson, A.A. Konnov, and M. Aldn. Photofragmentation laser-induced fluorescence imaging in premixed flames. *Combustion and Flame.*, 158:1908–1919, 2011.

[9] A. N. Karpetis and R. S. Barlow. Measurements of scalar dissipation in turbulent piloted methane/air jet flames. *Proc. Combust. Inst.*, 29:1929–1936, 2002.

[10] A. N. Karpetis and R. S. Barlow. Measurements of flame orientation and scalar dissipation in turbulent partially premixed methane flames. *Proc. Combust. Inst.*, 30:665–672, 2005.

[11] S. V. Kireev, S. L. Shnyrev, I. G. Simanovsky, I. V. Sobolevsky, S. V. Suganeev, and A. A. Kondrashov. A laser-induced fluorescence method for detecting iodine-129 in the atmosphere using a frequency-doubled neodymium laser. *Laser Phys.*, 23:105701, 2013.

[12] Malte Kllner, Penelope Monkhouse, and Jrgen Wolfrum. Time-resolved lif of oh in atmospheric-pressure flames using picosecond excitation. *Chemical Physics Letters.*, 168:355–360, 1990.

[13] Q.V. Nguyen, R.W. Dibble, C.D. Carter, G.J. Fiechtner, and R.S. Barlow. Raman-lif measurements of temperature, major species, oh, and no in a methane-air bunsen flame. *Combustion and Flame.*, 105:499–510, 1996.

[14] N. Peters. Laminar diffusion flamelet models in non-premixed turbulent combustion. *Prog. Eng. Combust. Sci.*, 10:319–339, 1984.

[15] J.A. Sutton and J.A. Driscoll. Scalar dissipation rate measurements in flames: A method to improve spatial resolution by using nitric oxide plif. *Proceedings of the combustion institute.*, 29:2727–2734, 2002.

[16] J.A. Sutton and J.A. Driscoll. A method to simultaneously image two-dimenstional mixture fraction, scalar dissipation rate, temperature and fuel consumption rate fields in a turbulent non-premixed jet flame. *Exp Fluids.*, 41:603–627, 2006.

[17] G. H. Wang and N. T. Clemens. Effects of imaging system blur on measurements of flow scalars and scalar gradients. *Exp. Fluids*, 37:194–205, 2004.

[18] Y.Zhao, C.Tong, and L.Ma. Assessment of a novel flow visualization technique using photodissociation spectroscopy. *Applied Spectroscopy.*, 63:199–206, 2009.

[19] Y.Zhao, C.Tong, and L.Ma. Demonstration of a new laser diagnostic based on photodissociation spectroscopy for imaging mixture fraction in a non-premixed jet flame. *Applied Spectroscopy.*, 64:377–383, 2010.

[20] Y.Zhao, C.Tong, and L.Ma. Kinetics of i2 and hi photodissociation with implications in flame diagnostics. *Applied Physics B.*, 104:689–698, 2011.

Participating Personnel

Chenning Tong: Professor (11/30/2014-03/30/2016)

Wei Li: Graduate student (11/30/2014-03/30/2016)

Mengyuan Yuan: Graduate student (11/30/2014-03/30/2016)

Publications resulted from this research

W. Li, M. Yuan, and C. Tong 2016 Simultaneous two-dimensional imaging of mixture fraction and temperature in turbulent partially premixed flames using a new laser diagnostic technique based on photodissociation and Rayleigh scattering. In preparation, to be submitted to *Combustion and Flame*.

1.

1. Report Type

Final Report

Primary Contact E-mail
Contact email if there is a problem with the report.

ctong@clemson.edu

Primary Contact Phone Number
Contact phone number if there is a problem with the report

864-656-7225

Organization / Institution name

Clemson University

Grant/Contract Title
The full title of the funded effort.

Experimental investigation of turbulence-chemistry interaction in high-Reynolds-number turbulent partially premixed flames

Grant/Contract Number
AFOSR assigned control number. It must begin with "FA9550" or "F49620" or "FA2386".

FA9550-14-1-0404

Principal Investigator Name
The full name of the principal investigator on the grant or contract.

Chenning Tong

Program Manager
The AFOSR Program Manager currently assigned to the award

Chiping Li

Reporting Period Start Date

09/30/2014

Reporting Period End Date

03/29/2016

Abstract

The project focused on implementing the photodissociation-based method for simultaneous two-dimensional imaging of mixture fraction and temperature in turbulent nonpremixed/partially premixed flames. Mixture fraction is an important variable in understanding and modeling turbulent mixing and turbulence-chemistry interaction, two key processes in such flames. Previous techniques are limited by one or more factors including the assumption of simplified flame chemistry, the use of non-inert tracer species, and the use of Raman scattering, thereby incapable of providing two-dimensional mixture fraction imaging in flames. Recently, a new method based on photodissociation of iodine containing species, two-photon laser-induced fluorescence (LIF) of atomic iodine, and Rayleigh scattering was developed by the PI and colleagues at Clemson University, enabling accurate simultaneous two-dimensional imaging in turbulent flames for the first time. The research activities focused on the technical issues in implementing the method, including achieving accurate iodine seeding level, eliminating the interference from LIF of molecular iodine excited at 532 nm and from OH excited at 298 nm, and determination of the system response. Two-dimensional imaging was performed in laminar and turbulent partially premixed methane flames to demonstrate the capability of the new measurement system.

Distribution Statement

This is block 12 on the SF298 form.

Distribution A - Approved for Public Release

Explanation for Distribution Statement

If this is not approved for public release, please provide a short explanation. E.g., contains proprietary information.

SF298 Form

Please attach your SF298 form. A blank SF298 can be found here. Please do not password protect or secure the PDF The maximum file size for an SF298 is 50MB.

Final_report2016.pdf

Upload the Report Document. File must be a PDF. Please do not password protect or secure the PDF . The maximum file size for the Report Document is 50MB.

IodineTPLIF.pdf

Upload a Report Document, if any. The maximum file size for the Report Document is 50MB.

Archival Publications (published) during reporting period:

None.

2. New discoveries, inventions, or patent disclosures:
Do you have any discoveries, inventions, or patent disclosures to report for this period?

No

Please describe and include any notable dates

Do you plan to pursue a claim for personal or organizational intellectual property?

Changes in research objectives (if any):

None.

Change in AFOSR Program Manager, if any:

None.

Extensions granted or milestones slipped, if any:

None.

AFOSR LRIR Number

LRIR Title

Reporting Period

Laboratory Task Manager

Program Officer

Research Objectives

Technical Summary

Funding Summary by Cost Category (by FY, $K)

	Starting FY	FY+1	FY+2
Salary			
Equipment/Facilities			
Supplies			
Total			

Report Document

Report Document - Text Analysis

Report Document - Text Analysis

Appendix Documents

2. Thank You

E-mail user

Jun 10, 2016 16:06:42 Success: Email Sent to: ctong@clemson.edu